

Contents list available at CBIORE journal website

Remarkable Energy Development

Journal homepage: https://ijred.cbiore.id



Research Article

Green intelligent building design based on integrated photovoltaic/thermal building

Tianchi Wang*

Faculty of Architecture and Civil Engineering, Huaiyin Institute of Technology, Huai'an, 223001, China

Abstract. With the increasingly prominent contradiction between energy consumption and environmental governance, the integrated photovoltaic/thermal building system has broad development prospects in building energy conservation. However, the improper placement of photovoltaic solar thermal collectors results in the inability of solar energy systems to maximize energy conversion. In order to combine photoelectric photothermal technology with architectural design, realize the efficient conversion and utilization of solar energy, reduce the dependence on traditional energy sources, and reduce building energy consumption, research based on the comprehensive utilization technology of solar photovoltaic photothermal building system, and optimized the system for different light resources and environmental conditions of solar photovoltaic photothermal building system, and optimized the system for different light resources and environmental conditions of solar photovoltaic photothermal collectors. The system achieved zero energy operation when the total energy consumption in winter was 798.92kW·h. The cumulative power supply and heat generation of the integrated photovoltaic/thermal building system throughout the winter were 214.63kW·h and 79.68kW·h. This study uses solar photovoltaic solar thermal collectors to replace roof coverings or insulation layers, which declines the impact of solar energy on buildings, and avoids duplicate investment and cuts cost. This study can improve power generation efficiency, meet heating needs, enhance resource utilization efficiency, reduce environmental pollution, and promote the sustainable development of the construction industry

Keywords: Photovoltaic/thermal building; Intelligent building; Green; Energy consumption; Energy saving design



@ The author(s). Published by CBIORE. This is an open access article under the CC BY-SA license (http://creativecommons.org/licenses/by-sa/4.0/).

Received: 5th Sept 2024; Revised: 9th January 2025; Accepted: 19th March 2025; Available online: 2nd April 2025

1. Introduction

Since industrialization, the construction industry worldwide has become one of the most energy intensive and carbon dioxide emitting sectors (Bacha et al. 2024). However, in the context of global warming, the construction industry is facing severe challenges such as environmental protection, energy conservation, and emission reduction. To address this challenge, achieving green and intelligent building systems has become a vital trend for sustainable development (Aryavalli and Kumar, Usman and Abdullah, 2023). The integrated Photovoltaic/Thermal (PV/T) building system is to install photovoltaic modules on the building facade, roof and other parts to fully utilize the surface space of the building, change solar energy into electrical energy, and achieve self-sufficiency of the building. In this system, photovoltaic thermal modules absorb solar energy, convert it into electrical energy, and generate thermal energy (Deng et al. 2024; Fakhabi et al. 2024). The hot and cold water pipelines are linked to a flat heat exchanger, through which the heat generated by solar energy is transferred to the water, and the heated water is then transported to a water tank for storage (Gatti et al. 2024). The direct current circulating water pump, battery, and inverter controller are responsible for managing and regulating the use and storage of electrical energy to ensure the stable operation. Auxiliary heating equipment provides additional thermal energy when necessary to ensure the efficiency and performance of the system (Panagiotidou et al. 2021). In practice, the integrated

PV/T building system can fully utilize the functions of solar water heaters to provide people with hot water for daily life or store thermal energy for heating, which can also provide some electricity (Hoxha *et al.* 2024; Hu *et al.* 2023). Therefore, the integrated PV/T building system has broad application prospects in building energy conservation. However, currently, traditional integration methods are mostly used for integrated PV/T building systems, which have problems such as limited installation area, unreasonable installation angle or orientation, shadow obstruction, and high component working temperature, which cannot fully utilize the advantages of high energy conversion efficiency (Liu *et al.* 2023; Olu-Ajayi *et al.* 2023).

Energy conservation needs to be considered in architectural design, but there are many factors related to building energy conservation design. Achieving optimal results for multiple factors at the same time is a problem worthy of longterm exploration. Existing technologies can solve the mutual constraints and contradictions between multiple objectives simulation, intelligent computer algorithm optimization, and other methods. Yu et al. (2023) conducted green intelligent building design on the ground of biological concepts, using the Deep Belief Network in to design a children's medical building. This strategy effectively detected human movements in multiple areas, and the lighting system could be automatically activated by pedestrians, which had positive impacts on people's emotions and achieved environmental therapy. In order to control indoor air pollution,

^{*} Corresponding author Email: wtianchi2024@163.com (W. Tang)

Lu et al. (2024) established a thermal and humidity coupling calculation model for porous fabrics. The Long Short-Term Memory (LSTM) was taken to input data. The LSTM prediction accuracy was better than that of Recurrent Neural Network (RNN), providing theoretical support for guiding and ensuring human health and safety. Ali et al. (2024) built a detailed analysis of the technical and non-technical losses of electricity based on machine learning in order to achieve efficient utilization of urban energy. Machine learning algorithms were combined with data balancing methods to improve electricity consumption detection. Different balancing methods had different impacts on the performance of classifiers. To enhance the quality of life and save energy, Akbarzadeh et al. (2023) used artificial intelligence algorithms for energy management. The LSTM-RNN was used to understand how to perform edge prediction on building energy, achieving performance of online monitoring models under various conditions. Zhang et al. (2024) proposed a theoretical framework for evaluating the cooperation capability of photovoltaic building materials on the basis of ecological reciprocity theory. They used field theory to establish a dynamic selection strategy for strategic alliance partners, combining decision rules with resource complementarity to improve the innovation efficiency.

In recent years, more scholars have begun to analyze the Energy Consumption (EC) characteristics of high-rise residential buildings and develop corresponding energy-saving strategies to achieve better energy-saving goals. Shahsavar et al. (2022) developed a multi criteria optimization algorithm for hybrid building integrated PV/T systems, with annual total power generation and fire consumption as objective functions. The optimized design generated rich energy, but the total energy generated was very low. The total power generation of systems with and without glass covers was approximately 227MWh and 220MWh, respectively. Miglioli et al. (2023) built a PV/T solar assisted heat pump system, which integrated a photovoltaic collector as the heat pump evaporator through synthesis methods, possible configurations, and design of subsystem components. This system achieved the highest heat recovery and performance, which met heating and cooling needs. Constantinou et al. (2024) compared the integrated photovoltaic configuration of buildings with existing solar photovoltaic systems. A path to enhance energy production and cost efficiency was drew as the key role. Exploring the interaction between energy efficiency and urban planning provides a comprehensive understanding of the various obstacles on the road to building integrated photovoltaic integration. Zadshir et al. (2023) designed a novel building integrated PV/T roof panel that considered both solar energy collection efficiency and thermal performance. Physical simulations of heat and mass transfer during operation were conducted using finite element method. The designed method lowered the surface temperature of solar modules from 88°C to 55°C. Therefore, reducing the output power from 14.89W to 10.69W could restore 30.2%. Da et al. (2023) combined photovoltaics with air source heat pumps to serve heating in non-centralized heating areas and created and numerically simulated thermal energy storage in TRNSYS. Compared with single heating, the synergistic effect of photovoltaics and air source heat pumps simultaneously improved the direct utilization rate of solar energy.

In summary, most research has focused on traditional EC monitoring and statistics, without adopting more scientifically accurate energy-saving strategies. In current building photovoltaic applications, the main focus is on power generation revenue, while neglecting the benefits of building energy efficiency. The building performance characteristics of

photovoltaic components, such as non transparency, low to medium transparency, and heat generation of component backboards in working conditions, if these characteristics are not fully utilized, will affect the integration effect of photovoltaic solar thermal buildings. In order to fully utilize the building performance characteristics of photovoltaic components, the research innovatively combines photovoltaic power generation, solar thermal utilization and other technologies with building design. It integrates year-round power generation, hot water, and passive heating/cooling, which not only meets the seasonal needs of buildings, reduces building cost, but also improves economic benefits.

Unlike previous studies that focused primarily on standalone photovoltaic or thermal systems, this study innovatively integrates photovoltaic power generation, solar thermal utilization, and passive building design into a unified system. Its novelty lies in three aspects: (1) The water-cooled PV /T collector replaces the traditional roof covering, eliminates the excess insulation layer, reduces the material cost, and improves the energy conversion efficiency. (2) A hybrid method combining TRNSYS transient simulation and Hooke-Jeeves algorithm is proposed to optimize the tilt Angle, azimuth Angle and collector area under dynamic environment conditions, which solves the limitations of static empirical model. (3) The system balances power generation and consumption through real-time energy management, achieving self-sufficiency in winter. The rationale for this approach is based on the need to address the tradeoff between energy efficiency and installation complexity. By utilizing computational optimization and modular design, the proposed system provides a scalable solution for different climate regions, in line with the United Nations Sustainable Development Goals (SDGS) on affordable and clean energy.

2. Experimental Procedure

The integrated PV/T building system is built. The complex subsystems of multiple components in the system are modeled by Transient System Simulation Program (TRNSYS) to optimize the energy performance and renewable energy systems.

2.1 Construction of mathematical model for integrated PV/T building system

A single solar cell module is usually composed of multiple individual solar cells connected in series. In practical applications, the back surface temperature of solar cell modules can reach 70°C in summer, and the working junction temperature of solar cells can reach 100°C. This results in an obvious decrease in the open circuit voltage of the component compared with its rated value, with a peak power loss rate of about 30%, and a significant decrease in output power with increasing temperature (Cao et al. 2023; Li et al. 2022). PV/T modules are a new integrated PV/T technology. The PV/T process involves laying liquid pipelines on the back side of the battery, which declines the operating temperature, and switch solar energy into electrical energy (Kaur et al. 2024). The cooling medium in the heat collection component can take away the heat from the battery for utilization, generating both electrical and thermal energy benefits. TRNSYS is an instantaneous system simulation program based on the Formula Translation (FORTAN), which can simulate PV/T systems, heat pump systems, air conditioning systems, etc (Lamichhane et al. 2024;

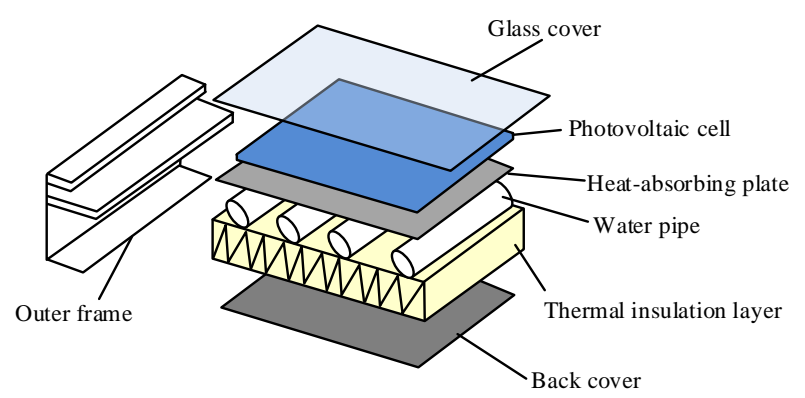


Fig 1 Water-cooled PV/T collector main structure

Li *et al.* 2024). There are numerous components in the integrated PV/T building system. Considering that water, air, electricity, and heat all have their own small systems, TRNSYS is used for transient simulation.

The water-cooled PV/T has the advantages of simple operation, no need for secondary heat exchange, good optical properties, high thermal capacity, and efficient utilization of low-grade thermal energy. Based on the PV/T collector, cold water can be introduced into the lower flow channel of the collector, and a part of the heat of the solar panel is swept up through heat exchange, lowering the solar panel temperature, thereby enhancing the photoelectric conversion efficiency, and generating hot water for use (Li and Zhong, 2024; Tang *et al.* 2024). Therefore, the study chooses it as the energy comprehensive utilization device module for modeling the integrated PV/T building system. The water-cooled PV/T collector is displayed in Figure 1.

This collector can produce hot water without consuming additional energy, because its design allows the system to generate electricity and hot water simultaneously through solar energy without increasing additional EC, making it significant advantages in energy conservation. The energy balance equation of water-cooled PV/T collectors is analyzed from four perspectives: glass cover plate, photovoltaic thermal material, flow channel water, and water storage tank. The theoretical calculation for the energy balance of glass cover plate is shown in equation (1).

$$\sigma_c \rho_g C_g \frac{dT_c}{dt} = G\alpha_g + (h_w + h_{ra})(T - T_c) + (h_{ge} + h_{rg})(T_e - T_c)$$
 (1)

In equation (1), σ_c signifies the cover plate thickness. ρ_g signifies the density of the cover plate. C_g represents the heat capacity of the cover plate. T_c represents the temperature of the glass panel. T represents the ambient temperature. h_{ge} represents the thermal convection coefficient. α_g represents the absorption rate of the glass cover plate. T_e represents the operating temperature of the PV/T collector. G represents the intensity of sunlight exposure. h_w signifies the thermal radiation coefficient of the component casing. h_{ra} signifies the thermal radiation coefficient between the component and the environment, and h_{rg} signifies the coefficient between the component and the solar panel. The energy balance of the entire system is displayed in equation (2).

$$\sigma_p \rho_c C_p \frac{dT_e}{dt} = WG\alpha_B - E + WG(h_{ge} + h_{rg})(T_c - T_e) + 8\pi r h_c (T_w - T_e) + W\frac{T_c - T_e}{R_{in}}$$
(2)

In equation (2), σ_p represents the thickness of the photothermal panel. W represents the width. ρ_c represents density. C_p represents the specific heat capacity of the photothermal panel. E represents the output power. T_w represents the average water temperature. h_c represents the heat transfer coefficient of the photovoltaic solar thermal panel. r represents the inner diameter of the tube. R_{in} signifies the back thermal resistance of the PV/T panel. The solar energy absorption rate α_B is displayed in equation (3).

$$\begin{cases} \alpha_{B} = \frac{\alpha_{p}[(1-\gamma)/(1+\gamma)]e^{-\lambda_{1}\sigma_{c}/\cos\theta_{2}}}{1-(1-\alpha_{p})\gamma} \\ \gamma = \frac{1}{2} \left[\frac{\sin^{2}(\theta_{2}-\theta_{1})}{\sin^{2}(\theta_{2}+\theta_{1})} + \frac{\tan^{2}(\theta_{2}-\theta_{1})}{\tan^{2}(\theta_{2}+\theta_{1})} \right] \end{cases}$$
(3)

In equation (3), α_p signifies the absorption rate of the photothermal panel. λ_1 represents the loss coefficient of sunlight in glass. θ_1 represents the angle of incidence of sunlight. θ_2 represents the refractive angle. The energy balance in a flowing channel is shown in equation (4).

$$\pi \left(\frac{r}{2}\right)^2 \rho_w C_w \frac{\partial T_w}{\partial t} = \pi r h_c (T_e - T_w) - m_w C_w \frac{\partial T_w}{\partial y} \tag{4}$$

In equation (4), ρ_w signifies the water density, and C_w signifies the specific heat capacity. m_w signifies flow velocity. The energy balance equation in the water tank is shown in equation (5).

$$M_t C_w \frac{dT_w}{dt} = N m_w \left(Tout_{min} ()_{t_t} (T - T_t) \right)$$
 (5)

In equation (5), M_t represents the capacity of the water reservoir. A_t represents the contact area. N signifies the drainage pipes. h_t signifies the heat transfer coefficient of the water reservoir. T_t represents the water temperature inside the reservoir. The PV/T collector utilizes the evaporation and condensation of heat pipes to exchange heat with the water in the reservoir. The total heat transfer coefficient U_A is shown in equation (6).

$$\frac{n}{U_A} = \frac{1}{h_0 A_0} + R_W + \frac{1}{h_i A_i} \tag{6}$$

In equation (6), h_0 and h_i are surface heat transfer coefficients used to describe the efficiency of heat exchange between the surface of an object and the fluid. n represents the number of heat exchange tubes. A_0 represents surface area and A_i represents internal surface area. R_w signifies the thermal resistance of the pipe wall, as displayed in equation (7).

$$R_W = \frac{\ln(r_0/r_i)}{2\pi L_p k_W} \tag{7}$$

In equation (7), r_0 signifies the outer diameter of the tube, and r_i signifies the inner diameter. L_p signifies the length of the tube node. k_w signifies the thermal conductivity of the heat exchanger wall. When there is no water flow in the heat exchanger, setting the Nusselt number to 1, the heat transfer between node j and node k in the heat storage tank can be calculated.

$$\begin{cases}
Q_{h,j\to k} = U_A (T_{tan k,j} - T_{h,k}) \\
Q_f = mC_p (T_{h,k} - T_{in})
\end{cases}$$
(8)

In equation (8), m represents the mass flow through the node. T_{in} represents the inlet temperature of the heat exchanger. $T_{h,k}$ represents the heat exchanger temperature. The rated pump power used in this system is very small, so factors such as starting, stopping, and pressure drop have little impact on the system performance. When the control signal received by the device is below 0.5, the pump stops working, and the output flow rate and energy transfer of the pump are both zero. The output liquid temperature is equal to that of the inlet liquid. When the input signal exceeds 0.5, the pump is turned on, and the mass flow of the pumped liquid and the power of the pump are set at the corresponding operating conditions. The efficiency for pumping fluid η_p is shown in equation (9).

$$\eta_p = \frac{\eta_o}{\eta_n} \tag{9}$$

In equation (9), η_o signifies the water pump's overall efficiency. η_n signifies the water pump motor efficiency. The pump shaft power P_s can be calculated using equation (10).

$$P_{\rm S} = P_r \times \eta_n \tag{10}$$

In equation (10), P_r signifies the rated power of the water pump. The energy Q transmitted from the water pump motor to the fluid can be calculated by equation (11).

$$Q = P_{S}(1 - \eta_{n}) + (P - P_{S})f \tag{11}$$

In equation (11), f represents the efficiency loss ratio of the motor, including hydraulic loss, volume loss, and mechanical loss. The energy transmitted by the water pump motor to the surrounding environment can be calculated using equation (12).

$$Q_a = P_r(1 - \eta_n)(1 - f_m) \tag{12}$$

In equation (12), Q_a represents the energy transmitted by the water pump motor to the surrounding environment. The outlet

fluid temperature $T_{f,out}$ of the water pump is shown in equation (13).

$$T_{f,out} = T_{f,in} + \frac{Q}{m} \tag{13}$$

In equation (13), $T_{f,in}$ represents the inlet fluid temperature of the water pump.

2.2 Optimization of integrated photovoltaic/thermal building system

The efficient operation of PV/T components can reduce dependence on traditional power systems, thereby reducing EC and carbon emissions. Therefore, the integrated photovoltaic and thermal building system is optimized. The water-cooled photovoltaic integrated building consists of a water circulation system and a photovoltaic power generation system. Solar radiation can effectively control the temperature of photovoltaic cells, thereby enhancing the efficiency of photovoltaic implementation and effectively utilizing waste heat, as displayed in Figure 2 (Wakil et al. 2024; Wei et al. 2023). PV/T modules utilize the photoelectric effect of semiconductors to directly convert sunlight into electrical energy. They are installed in suitable locations of buildings, such as roofs or walls, to receive sunlight. The captured solar radiation heat is applied to heat water or other fluids, provide hot water supply or space heating.

Under the premise of unchanged area and external light intensity, adding the receiving area of the PV/T collector can improve its heat generation capacity, and achieving maximum solar radiation through reasonable arrangement and installation angles (Zhang *et al.* 2024). At noon, facing the sun directly to obtain the maximum solar radiation energy. In theory, if the inclination angle of the module is consistent with the local latitude, the photovoltaic/T module will receive the highest total solar radiation in a year (Mohkam *et al.* 2023; Zhang, 2024), as shown in Figure 3.

According to Figure 3, the theoretical optimal inclination angle of the inclined surface component is shown in equation (14).

$$\theta = 180^{\circ} - 90^{\circ} - \alpha_{se} \tag{14}$$

In equation (14), θ represents the optimal inclination angle. α_{se} represents the altitude angle of the sun, as shown in equation (15).

$$\alpha_{se} = 90^{\circ} - D_{\text{dimensionality}}$$
 (15)

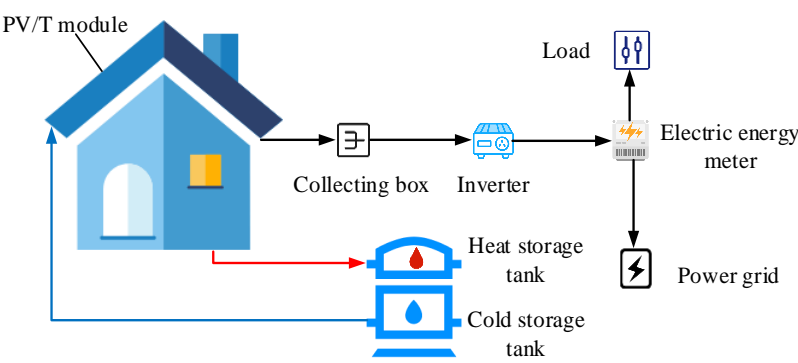


Fig 2 Structure diagram of water-cooled photoelectric integrated building

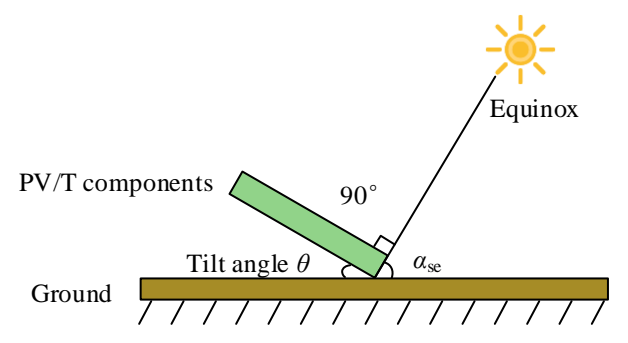


Fig 3 PV/T component installation diagram

In equation (15), $D_{\rm dimensionality}$ represents the dimension. Based on the energy balance equation and system performance parameters, the objective function shown in equation (16) can be obtained.

$$\begin{cases} f = \frac{1}{P_{\text{gen}} + Q_{\text{gen}}} \\ P_{\text{gen}} = \eta_{\text{pv}} \cdot G_{\text{horizontal}} \cdot \cos(\alpha_{se}) \cdot A \\ Q_{\text{gen}} = \eta_{\text{th}} \cdot G_{\text{horizontal}} \cdot \cos(\alpha_{se}) \cdot A \end{cases}$$
(16)

In formula (16), $P_{\rm gen}$ is the system power generation; $\eta_{\rm pv}$ is the efficiency of photovoltaic modules, taking 15%; $G_{\rm horizontal}$ is the amount of solar radiation on the horizontal plane; $Q_{\rm gen}$ is the system heat yield; $\eta_{\rm th}$ is the heat collection efficiency, which is 50%.

The study selects the Generic Optimization Program (GenOpt) to optimize the tilt angle, and other parameters of the solar cell collector plate. This program can be accessed through the Transient System Optimization (TRNOpt) in the Energy Systems Simulation (TESS) program. The GenOpt program can only solve the minimum value problem. By minimizing the inverse of the sum of system power generation and heat

generation, the optimization objective can be indirectly achieved, which is to maximize the total system power generation and heat generation. This transformation is a common method in mathematical optimization, which changes the sign and type of the objective function to make problems that were originally difficult to handle directly solvable. The Hooke-Jeeves algorithm is an algorithm for solving unconstrained optimization problems, which does not require calculating the derivative of the objective function (Ly and El-Sayegh, 2023). Therefore, the Hooke-Jeeves optimization algorithm is selected to solve this problem. The advantage of Hooke-Jeeves algorithm is that it does not require solving the second derivative or Jacobi matrix of the problem, which makes it advantageous in dealing with some complex or difficult to analyze nonlinear problems with second derivatives.

The calculation flowchart of Hooke-Jeeves algorithm is displayed in Figure 4. The objective function is f(x), and $x \in \mathbb{R}^n$. The coordinate directions is $e_i = (0, \cdots, 0, 1, 0, \cdots, 0)^T$, and $i = 1, \cdots, n$. The initial step size is δ . The acceleration factor is a. The step shortening coefficient is w and the accuracy value is ε . Any starting point x_1 is selected as the first base point. x_i represents the i-th base point. In each detection search, y represents the independent variable, that is, the starting point of the detection along e_i is y_i . y_{n+1} is the point detected along e_n (Garai et al. 2023).

In this study, a transient system simulation program based on TRNSYS was used to build a PV/thermal integrated building system model, and multi-parameter optimization of the system was carried out by GenOpt optimization software combined with Hooke-Jeeves algorithm. The initial step size of the algorithm is set to 1, the acceleration factor is 1.2, the step shortening coefficient is 0.5, the convergence accuracy is 5×10⁻³, and the maximum number of iterations is 500. First, the initial value of the variable is initialized and the value of the objective function is calculated. Then the probe search is carried out along each variable direction to update the variable value. If the value of the objective function decreases, the search is accelerated. Otherwise shorten the step length. Repeat the

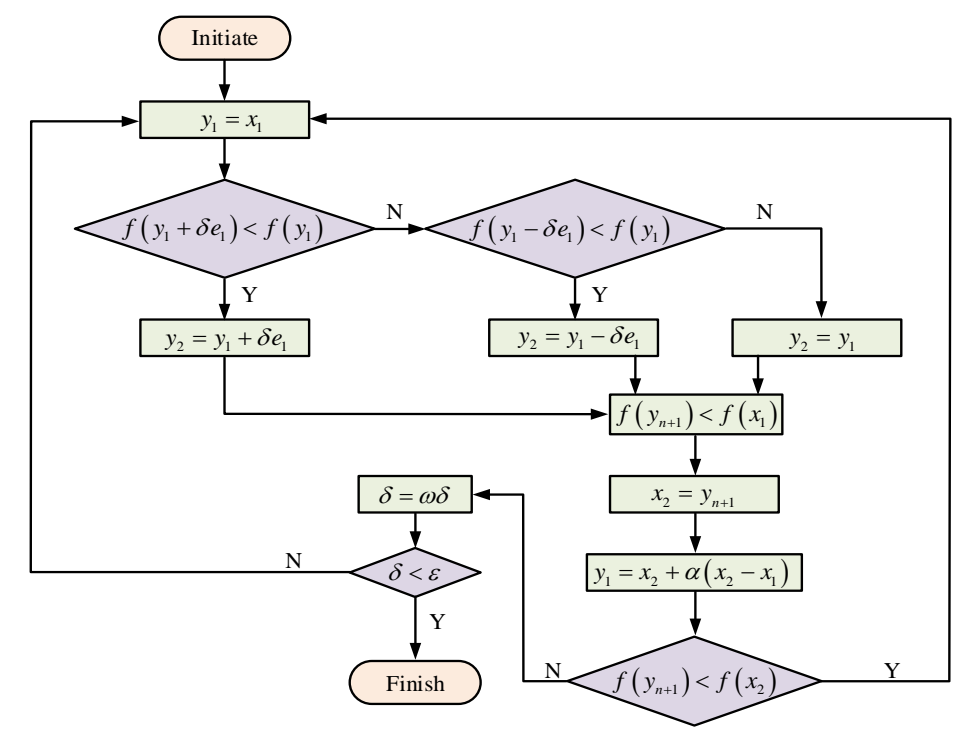


Fig 4 Calculation flow diagram of Hooke-Jeeves algorithm

above steps until the convergence condition is met. In the optimization process, TRNSYS simulates the system performance under different parameter combinations, and GenOpt iteratively adjusts the parameters to approximate the optimal solution.

3. Result and Discussion

The performance of the integrated PV/T building system in winter is analyzed. The PV/T is optimized from the optimal azimuth and installation angle, as well as the collector area. A comprehensive analysis is conducted on the performance comparison with a single PV system, including environmental and economic benefits.

3.1 System performance analysis

In GenOpt software, all variables involved are selected as continuous numerical types. In the variable settings menu, the initial value is 150, the minimum is 100, the maximum is 600, the step size is 1, and the objective function is set with "Use Equation". Due to too few iterations or low computational accuracy, the objective function may not converge, resulting in optimization failure. Excessive repetition can lead to high accuracy, resulting in slower optimization speed and redundant operations. Therefore, in this optimization setting, 500 iterations are conducted with an accuracy of 5.

The study uses Pvsyst software to simulate and analyze the optimal azimuth and installation angle for specific areas, as

shown in Figure 5. There is an inclination angle that allows the inclined surface to receive the maximum solar radiation. The annual total radiation of 1264 kWh/m² aligns with findings by Wagle *et al.* (2024), who emphasized the role of tilt angle optimization in urban PV systems. Therefore, in the integrated PV/T building system, to ensure the maximum annual total solar radiation, the tilt angle should be set to 15°.

Optimizing the area of PV/T collectors is one of the key steps to optimize the efficiency of solar photovoltaic cogeneration systems. By adjusting the area of the collector, the system's power generation and consumption can be better matched, thereby improving energy efficiency. The system can meet energy demand while minimizing energy waste, optimizing the overall performance and economic benefits. The areas of 9 different PV/T collectors are selected, with increases of 2m² in sequence. After several simulations in the TRNSYS system editing interface, the simulation results shown in Figure 6 are obtained. As the area increases, the collected heat and the cumulative power generation also increased accordingly, lowering the total EC. When the PV/T collector area was 16m², the total EC was 798.92kW·h, and the system's power generation and total EC were equal, achieving self-sufficiency in electricity consumption. The total EC in winter was zero.

Figure 7 shows the hourly indoor temperature and outdoor temperature during winter. During the heating period, the average indoor temperature was 23.84°C. Compared with the average outdoor temperature of 1.89°C, the temperature difference between indoor and outdoor reached 21.95°C. Referring to the regulation in the centralized heating regulations

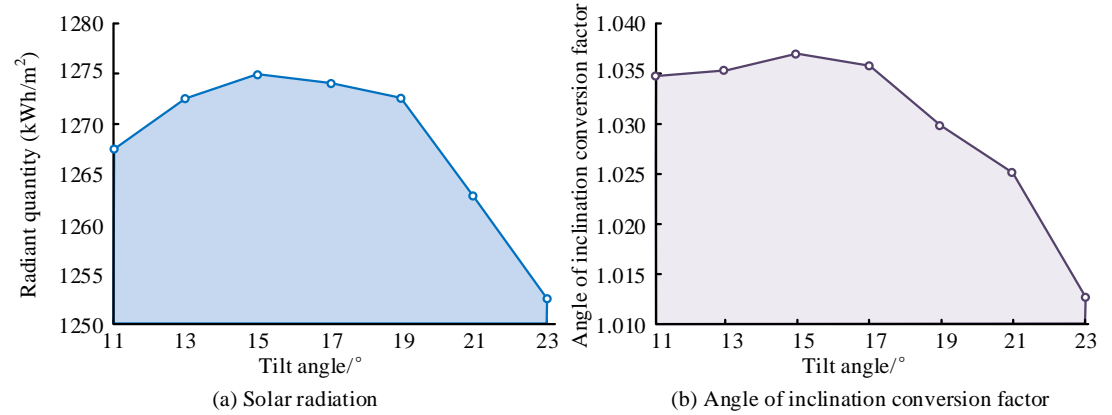


Fig 5 Solar radiation at different tilt angles

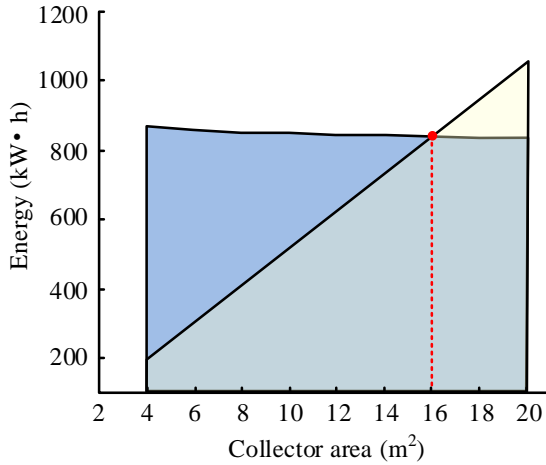


Fig 6 Cumulative power generation and total energy consumption as a function of PV/T collector area

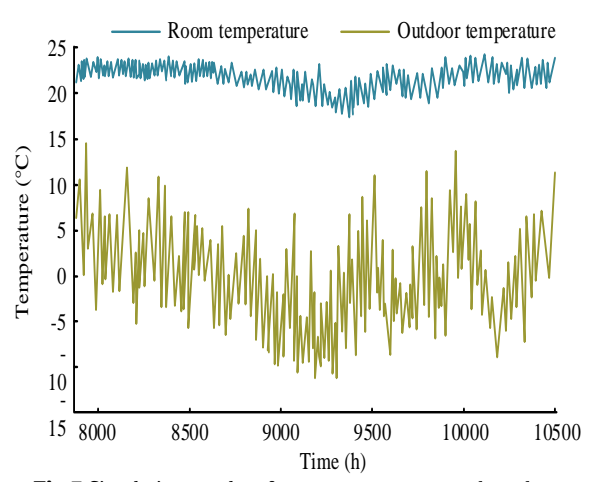


Fig 7 Simulation results of room temperature and outdoor temperature

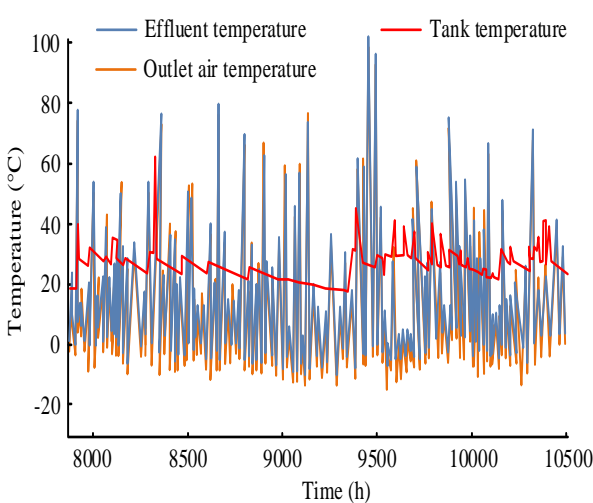


Fig 8 Hourly output temperature of system components

of the region that "heating enterprises should ensure that the indoor temperature of users' bedrooms and living rooms is not less than 18°C", the heating effect of the system is better. In the case of outdoor minimum -10.68°C, the indoor temperature was above 18 °C, which met the needs of indoor heating.

Figure 8 displays the hourly output temperature of each component of the system during winter. When the average outdoor temperature was 1.95°C and the average heating air temperature was 25.28°C, it indicated that the system could achieve good heating effect in winter. The temperature difference of building water supply was 19.21°C, which could

effectively preheat domestic hot water, reduce the EC, and have a certain energy-saving effect.

Figure 9 displays the simulation results of cumulative power consumption and remaining power. From Figure 9 (a), the power consumption steadily increased over time, due to the intermittent nature of the system in the simulated operating state. The heating at night was mainly auxiliary heating, which required continuous power supply from the urban power grid. The emergence of surplus electricity is due to the instantaneous generation of sufficient power to meet the immediate electricity needs of necessary electrical devices. The surplus electricity can be stored in energy storage modules and used on other small electrical devices. The amount of such electricity is very small, and the accumulated surplus electricity is also very small. Overall, the total power supply in winter was 701.36kW·h, with a surplus of 60.12kW·h. Figure 9 (b) shows the cumulative heat generation and power generation in winter. The changes in cumulative heat generation and power generation over time can be divided into three periods. In the first phase (8000-9000 hours), affected by the continuous increase in solar radiation intensity, the energy absorbed by the system also increased, and the cumulative heat production and heat production gradually increased. In the second phase (9000-9500 hours), the cumulative heat value and power generation increased slowly. Especially during this stage, due to the lower average outdoor temperature and higher EC, the cumulative heat value increased to 0. The third phase was 9500-10500 hours, and the cumulative heat production and power generation increased again. In summary, the cumulative power supply during winter is 214.63kW·h, and the cumulative heat generation is 79.68kW·h.

3.2 Energy-saving effect analysis

To verify the energy-saving effect of the proposed system, a simulation analysis is conducted on the monthly power generation in winter. The results are shown in Figure 10. The system's power generation reached its maximum value in December and January, with 54.63kW·h and 52.14kW·h, respectively. This is mainly because the gradual increase in solar radiation and the gradual decrease in external temperature during this period, resulting in a significant temperature difference and increased heat generation. From mid January to mid February, the power generation and heat generation decreased by 28.54kW·h and 16.74kW·h, respectively. The reason for this is that during this period, the increased external temperature lowers temperature gradient. The increase or decrease in power generation and heat generation is close, indicating the effectiveness of the comprehensive utilization efficiency of the system proposed in the study.

Figure 11 shows the EC and total power generation for each month in winter. Comparing the EC of auxiliary heating in Figures 11 (a) and 11 (b) with the total EC, the EC of auxiliary

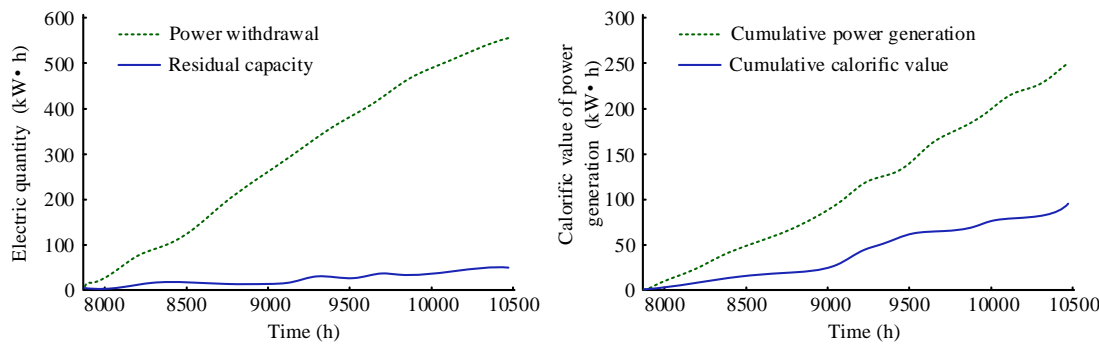


Fig 9 Power generation simulation results

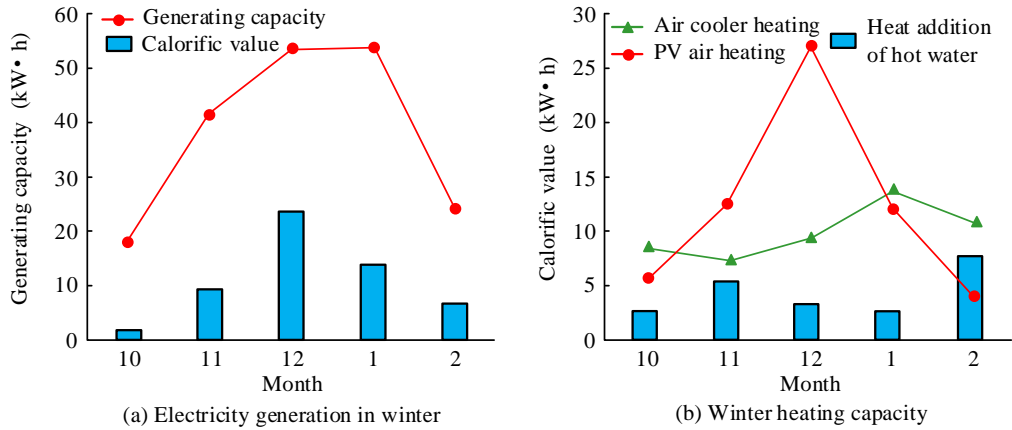


Fig 10 Monthly energy generation in winter

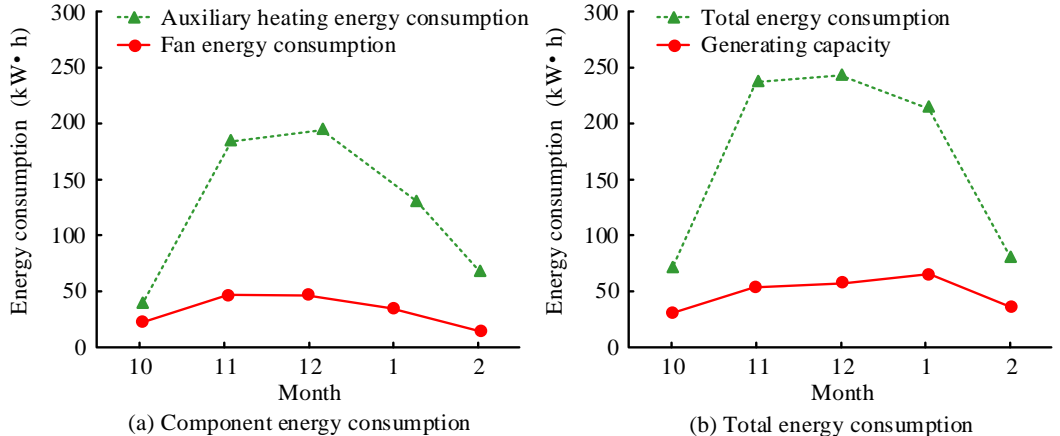


Fig 11 Monthly EC and total monthly power generation

heating exceeded 80% of the total EC of the system, which was a vital element affecting the EC of the entire system. Taking the difference between the total EC and power generation points in Figure 11(b), the energy saving rates for each month in winter were 16.82%, 17.26%, 19.71%, 26.91%, and 33.67%. The energy-saving rate of 33.67% in February surpasses the 25% reported by Obeidat *et al.* (2024), likely due to the integration of passive heating strategies (Qian *et al.* 2024). The system can effectively utilize electricity and save a certain amount of energy.

December 15th, which is closer to the middle of the heating season, is selected as the typical working day of the heating season. The TRNSYS model is used to conduct numerical simulations from December 15th to December 16th. The simulation step size is adjusted to 1 hour. Figure 12 displays the relationship between indoor temperature and heating air temperature under typical winter working conditions. The average indoor temperature was maintained at around 20°C throughout the day. The system can work normally during the heating period. The comprehensive utilization rate of

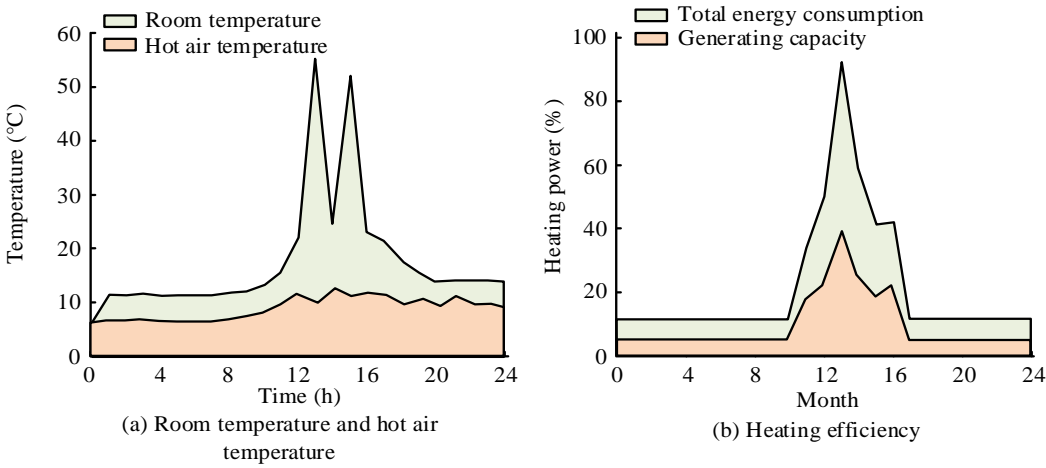


Fig 12 typical working condition of the simulation results

Table 1Comparison of other works

Study	System Type	Power Generation (kW·h)	Heat Generation (kW·h)	Energy Saving Rate	Key Innovation
Lachir <i>et al.</i> (2022)	PV/T with glass cover	227 MWh/year	180 MWh/year	18%	Hybrid PV/T and heat exchanger
Zhang <i>et al.</i> (2023)	Novel PV/T roof panel	14.89 W/m²	10.69 W/m²	25%	Reduced module temperature by 33°C
This study	Integrated PV/T	214.63 (winter)	79.68 (winter)	26.91% (avg)	Zero-energy operation at 16 m ² collector area

photovoltaics and photothermal is high, which can reduce the consumption of traditional primary energy, reduce heating costs, and have important significance for energy conservation and environmental protection.

Table 1 shows the results of comparison with other works. As can be seen from the table, the study of Lachir et al. (2022) adopted a PV/T system with 227 glass covers, with an annual generating power of 227 MWh, thermal generation into 180 MWh, and an energy saving rate of 18%. The key innovation lies in the combination of hybrid PV/T and heat exchanger. Zhang et al. (2023) developed a new PV/T roof panel with a generating power of 14.89 W/m² and thermal generation to 10.69 W/m², which achieved a 25% temperature reduction by reducing the module temperature by 33°C. The key innovation is to reduce the module temperature to achieve zero energy operation. In this study, an integrated PV/T system was constructed. In winter, the generating power reached 214.63 kW·h, the thermal generation became 79.68 kW·h, and the average energy saving rate was 26.91%. The main innovation was to achieve zero energy consumption operation on the collector area of 16 m². On the whole, this study is superior to the previous two studies in terms of power generation, heat generation and energy saving rate, and has achieved zero energy consumption operation on a small collector area, showing high efficiency and innovation.

4. Conclusion

This study proposes an integrated photovoltaic/thermal (PV/T) building system that synergizes photovoltaic power generation and solar thermal utilization to address the inefficiencies of traditional PV/T systems. By optimizing the tilt angle, azimuth, and collector area, the system achieves zero-energy operation during winter, significantly reducing reliance on auxiliary heating. The integration of water-cooled PV/T collectors with building design not only enhances energy conversion efficiency but also eliminates redundant insulation layers, offering a cost-effective and sustainable solution for building energy conservation.

Compared to conventional PV systems, the proposed design demonstrates superior energy efficiency and resource utilization, aligning with global goals for carbon neutrality and sustainable development. Future research should focus on integrating IoT-based real-time monitoring and multi-objective optimization to further improve system performance and address component-level cost and performance trade-offs. This approach has the potential to revolutionize building energy systems, particularly in regions with high heating demands, by providing a scalable and environmentally friendly solution. In this study, the PV/T installation parameters considered in the

design process are less, and in the actual project, the power consumption, size and price of each component are also important factors affecting the system performance. In the future, real-time monitoring and optimization of building energy consumption and equipment operation should be realized through technologies such as the Internet of Things to further improve the green performance of the building.

References

- Akbarzadeh, O., Hamzehei, S., Attar, H., Amer, A., Fasihihour, N., Khosravi, M. R., et al. (2023). Heating-cooling monitoring and power consumption forecasting using lstm for energy-efficient smart management of buildings: A computational intelligence solution for smart homes. *Tsinghua Science and Technology*, 29(1): 143-157. https://doi.org/10.26599/tst.2023.9010008
- Ali, A., Khan, L., Javaid, N., Aslam, M., Aldegheishem, A., Alrajeh, N. (2024). Exploiting machine learning to tackle peculiar consumption of electricity in power grids: A step towards building green smart cities. *IET Generation, Transmission & Distribution*, 18(3): 413-445. https://doi.org/10.1049/gtd2.13056
- Aryavalli, S. N. G., Kumar, G. H. (2023). Futuristic vigilance: Empowering chipko movement with cyber-savvy IoT to safeguard forests. *Archives of Advanced Engineering Science*, 1(8): 1-16. https://doi.org/10.47852/bonviewaaes32021480
- Bacha, B., Rebah, N., Sengouga, N. (2024). Energy and parametric analysis of solar absorption cooling systems for an office building: a case study. *Energy Sources, Part A: Recovery, Utilization, and Environmental Effects,* 46(1): 6794-6815. https://doi.org/10.2139/ssrn.4494898
- Cao, H., Wu, Y., Bao, Y., Feng, X., Wan, S., Qian, C. (2023). UTrans-Net:

 A model for short-term precipitation prediction. *Artificial Intelligence and Applications*, 1(2): 106-113. https://doi.org/10.47852/bonviewaia2202337
- Constantinou, S., Al-naemi, F., Alrashidi, H., Mallick, T., Issa, W. (2024).

 A review on technological and urban sustainability perspectives of advanced building-integrated photovoltaics. *Energy Science & Engineering*, 12(3): 1265-1293. https://doi.org/10.1002/ese3.1639
- Da, J., Li, M., Li, G., Wang, Y., Zhang, Y. (2023). Simulation and experiment of a photovoltaic—air source heat pump system with thermal energy storage for heating and domestic hot water supply. *Building Simulation*, 16(10): 1897-1913. https://doi.org/10.1007/s12273-022-0960-6
- Deng, Q., Li, H., Pei, K., Wong, L. W., Zheng, X., Tsang, C. S., et al. (2024). Strategic Design for High-Efficiency Oxygen Evolution Reaction (OER) Catalysts by Triggering Lattice Oxygen Oxidation in Cobalt Spinel Oxides. ACS nano, 18(49): 33718-33728. https://doi.org/10.1021/acsnano.4c14158.s001
- Fakhabi, M. M., Hamidian, S. M., Aliehyaei, M. (2024). Exploring the role of the Internet of Things in green buildings. *Energy Science & Engineering*, 12(9): 3779-3822. https://doi.org/10.1002/ese3.1840
- Gatti, C., Lodi, C., Muscio, A. (2024). Conventional Building Energy Performance and Actual Energy Costs: A Critical Reflection.

- International Journal of Sustainable Development and Planning, 19(10): 3707-3714. https://doi.org/10.18280/ijsdp.191001
- Garai, S., Paul, R. K., Kumar, M. (2023). Intra-annual national statistical accounts based on machine learning algorithm. *Journal of Data Science and Intelligent Systems*, 2(2): 12-15. https://doi.org/10.47852/bonviewjdsis3202870
- Hoxha, V., Dinçer, H., Yuksel, S. (2024). Analysis of strategic priorities of green building projects for the efficient energy consumption. *International Journal of Energy Sector Management*, 18(6): 1221-1243. https://doi.org/10.1108/ijesm-05-2023-0015
- Hu, C., Liu, P., Yang, H., Yin, S., Ullah, K. (2023). A novel evolution model to investigate the collaborative innovation mechanism of green intelligent building materials enterprises for construction 5.0. AIMS Math, 8(4): 8117-8143. https://doi.org/10.3934/math.2023410
- Kaur, L., Kaur, R. (2024). Fog-Based Energy Efficient Routing Protocol for Smart Building Evacuations. Wireless Personal Communications, 139(1): 543-571. https://doi.org/10.1007/s11277-024-11637-8
- Lachir, A., Noufid, A. (2024). Assessment of building design strategies to enhance energy efficiency and thermal comfort: Case study in Morocco's climate zones. *Journal of Building Physics*, 48(2): 197-221. https://doi.org/10.1177/17442591241266608
- Lamichhane, S., Mostafa, R., Gopalakrishnan, B. (2024). An eQUEST Based Building Energy Modeling Analysis for Energy Efficiency of Buildings. *Energy Engineering*, 121(10): 2743-2767. https://doi.org/10.33915/etd.8266
- Li, J., Zhang, C., Zhao, Y., Qiu, W., Chen, Q., Zhang, X. (2022).

 Federated learning-based short-term building energy consumption prediction method for solving the data silos problem.

 Building Simulation, 15(6):1145-1159. https://doi.org/10.1007/s12273-021-0871-y
- Li, L., Qi, Z., Ma, Q., Gao, W., Wei, X. (2024). Evolving multi-objective optimization framework for early-stage building design: Improving energy efficiency, daylighting, view quality, and thermal comfort. Building Simulation. *Beijing: Tsinghua University Press*, 17(11): 2097-2123. https://doi.org/10.1007/s12273-024-1178-6
- Liu, K., Sun, Y., Yang, D. (2023). The administrative center or economic center: Which dominates the regional green development pattern. A case study of Shandong peninsula urban agglomeration, China. *Green and Low-Carbon Economy*, 1(3), 110-120. https://doi.org/10.47852/bonviewglce3202955
- Li, Y., Zhong, H. (2024). Construction and Research of Water Reuse System in Green Intelligent Buildings. Archives des Sciences, 74(1): 92-101. https://doi.org/10.62227/as/74112
- Lu, L., Huang, X., Zhou, X., Guo, J., Yang, X., Yan, J. (2024). High-performance formaldehyde prediction for indoor air quality assessment using time series deep learning. *Building Simulation*, 17(3): 415-429. https://doi.org/10.1007/s12273-023-1091-4
- Ly, A., El-Sayegh, Z. (2023). Tire wear and pollutants: An overview of research. *Archives of Advanced Engineering Science*, 1(1): 2-10. https://doi.org/10.47852/bonviewaaes32021329
- Miglioli, A., Aste, N., Del Pero, C., Leonforte, F. (2023). Photovoltaic-thermal solar-assisted heat pump systems for building applications: Integration and design methods. *Energy and Built Environment*, 4(1): 39-56. https://doi.org/10.1002/9781394249374.ch22
- Mohkam, M., Mohammadi, S. M, H., Arababadia, R., Jahanshahi, Javaran. (2023). Impacts of phase change materials on performance of operational peak load shifting strategies in a sample building in hot-arid climate. *Environmental Progress & Sustainable Energy*, 42(1):13961-13990. https://doi.org/10.1002/ep.13961
- Obeidat, L. M., Jones, J. R., Mahaftha, D. M., Amhamed, A. I., Alrebei, O. F. (2024). Optimizing indoor air quality and energy efficiency in multifamily residences: Advanced passive pipe system parametrics study. *International Journal of Environmental Science and Technology*, 21(16): 10003-10026. https://doi.org/10.1007/s13762-024-05624-6

- Olu-Ajayi, R., Alaka, H., Owolabi, H., Akanbi, L., Ganiyu, S. (2023). Data-driven tools for building energy consumption prediction: A review. *Energies*, 16(6): 2574-2598. https://doi.org/10.3390/en16062574
- Panagiotidou, M., Brito, M., Hamza, K., Jasieniak, J., Zhou, J. (2021).

 Prospects of photovoltaic rooftops, walls and windows at a city to building scale. *Solar Energy*, 230(12):675-687. https://doi.org/10.1016/j.solener.2021.10.060
- Qian, K. (2024). Optimization Algorithm for Green Environment Design Based on Artificial Intelligence. *Scalable Computing: Practice and Experience*, 25(5): 3547-3553. https://doi.org/10.12694/scpe.v25i5.3123
- Shahsavar, A., Arici, M. (2022). Effect of glass cover on the energy and exergy performance of a combined system including a building integrated photovoltaic/thermal system and a sensible rotary heat exchanger. *International Journal of Energy Research*, 46(4): 5050-5066. https://doi.org/10.1002/er.7499
- Tang, B., Song, F., Wu, J. M., Tan, Q. W., Zhao, Y. Y., Zhou, J., et al. (2024). A Mussel-Inspired and Recyclable Coating with Integrated Daytime Radiative Cooling and Triboelectric Energy Harvesting for Intelligent and Sustainable Buildings. ACS Applied Materials & Interfaces, 16(41): 56159-56169. https://doi.org/10.1021/acsami.4c12693.s001
- Usman, A. M., Abdullah, M. K. (2023). An assessment of building energy consumption characteristics using analytical energy and carbon footprint assessment Model. *Green and Low-Carbon Economy*, 1(1): 28-40. https://doi.org/10.47852/bonviewglce3202545
- Wagle, S., Gopalakrishnan, B., Li, H., Liu, Z., Chaudhari, S., Sundaramoorthy, S. (2024). Simulating energy performance of buildings: a study using eQUEST and Energy Star® portfolio manager. *Architectural Engineering and Design Management*, 20(5): 997-1018. https://doi.org/10.33915/etd.12123
- Wakil, M., El, Mghari H., Kaitouni, S. I., Amraoui, El. R. (2024). Thermal energy performance of compressed earth building in two different cities in Moroccan semi-arid climate. *Energy and Built Environment*, 5(5): 800-816. https://doi.org/10.1016/j.enbenv.2023.06.008
- Wei, G., Sarman, A. M., Li, M., Shen, L. (2023). A comprehensive approach for thermal comfort analysis in green intelligent buildings using BIM technology. *Journal of System and Management Sciences*, 13(2): 515-528. https://doi.org/10.33168/jsms.2023.0235
- Yu, T., Yang, X., Sang, P. (2023). Design strategy of green intelligent building using deep belief network. International Journal of System Assurance Engineering and Management, 2023, 14(1): 196-205. https://doi.org/10.1007/s13198-021-01513-0
- Zadshir, M., Wu, C., Yu, X., Yin, H. (2023). Design and performance testing of a novel building integrated photovoltaic thermal roofing panel. *Building Simulation*, 16(10): 1863-1879. https://doi.org/10.1007/s12273-023-1027-z
- Zhang, D., Li, Q., Fang, Y., Bai, P., Liu, L., Guo, J., et al. (2024). Highperformance wood-based thermoelectric sponges for thermal energy harvesting and smart buildings. *Nano Research*, 17(6): 5349-5357. https://doi.org/10.1007/s12274-024-6467-y
- Zhang, N., Yin, J., Zhang, N., Sun, T., Yin, S., Wan, L. (2024). Artificial intelligence-driven photovoltaic building materials industry: Greenization and digitization innovation conversion of photovoltaic technology based on a novel interval fuzzy field theory decision-making model. *Journal of Intelligent & Fuzzy Systems*, 46(3): 6411-6437. https://doi.org/10.3233/jifs-234838
- Zhang, X., Ning, Q., Chen, Z. (2023). Multi-objective optimization design of energy efficiency for office building window systems based on indoor thermal comfort. Science and Technology for the Built Environment, 29(6): 618-631. https://doi.org/10.1080/23744731.2023.2194840
- Zhang, Y. (2024). Research on the Application of Artificial Intelligence-based Cost Estimation and Cost Control Methods in Green Buildings. Scalable Computing: Practice and Experience, 25(6): 4772-4779. https://doi.org/10.12694/scpe.v25i6.3293



© 2025. The Author(s). This article is an open access article distributed under the terms and conditions of the Creative Commons Attribution-ShareAlike 4.0 (CC BY-SA) International License (http://creativecommons.org/licenses/by-sa/4.0/)